Proceedings of the 21st ICSMGE, Vienna, Austria, 14 – 19 June 2026. Pistrol, Adam & Schweiger (eds.)
Published by: ÖGG, Austrian Society for Geomechanics, Salzburg, Austria, ISBN 978-3-9503898-4-5
https://doi.org/10.53243/ICSMGE2026-347

Stability of Tunnel in Spatially Variable Cohesive Frictional Soils using Random Finite Element Limit Analysis

Siddharth Pandey
Department of Civil Engineering, Research Scholar, Indian Institute of Technology Roorkee, India 247667

Akanksha Tyagi
Department of Civil Engineering, Assistant Professor, Indian Institute of Technology Roorkee, India, 247667, akanksha.tyagi@ce.itr.ac.in

ABSTRACT: The spatial variation in the soil properties often results in highly heterogeneous ground profiles. In this study, random finite element limit analysis (RFELA) is performed to study the effect of the isotropic and anisotropic spatial variability of the surrounding cohesive frictional lateritic soil on the stability of the tunnel. The effect of random fields of effective cohesion (c'), effective friction angle (ϕ'), and unit weight (γ) considering isotropic and anisotropic correlation length (CL) are studied for a 6 m diameter tunnel at a cover depth to diameter ratio of 1. Parametric studies have been conducted to analyze the effects of varying the coefficient of variation (COV), horizontal and vertical correlation length i.e. CL_H and CL_V on the probability of failure (P_f). The probability density functions and the cumulative distribution functions of the tunnel collapse pressures for various cases are presented. Finally, values of P_f are calculated for the various cases, and are also compared with those from the random finite element analysis.

KEYWORDS: Tunnel, c'-ϕ' soil, random field, limit analysis, probability of failure.

1 INTRODUCTION

Tunnel construction has always been associated with complex geology, geotechnical profiles, and terrains. Inadequate design and analysis of tunnels lead to catastrophic failure (Imteyaz and Mishra 2023). In the past, researchers (Sloan and Assadi 1993; Zhang et al. 2016) conducted tunnel stability analyses for a range of geotechnical profiles as well as for different geometrical parameters. These studies proposed stability charts, and failure mechanisms associated with tunnel stability. It is well known that the process of soil formation is associated with various continuous physico-chemical processes (Campbell 1979). The combined action of these processes gives rise to inherent uncertainties and heterogeneity in the soil profile. Due to the heterogeneous nature of soil, geotechnical properties exhibit variation both horizontally and vertically, resulting in a spatially variable soil profile. Therefore, no geotechnical profile is completely free from uncertainty (Curran and Hammah 2006). Conventional deterministic tunnel stability analyses do not consider the uncertainties associated with soil parameters and therefore overpredict the stability and performance of tunnels (Hamrouni et al. 2022). Methods such as the first-order reliability method (Low and Einstein 2013) and Monte Carlo simulations (Vargas et al. 2014) are employed to account for the uncertainties associated with soil parameters; however, these methods do not incorporate the spatial variability of soils. These methods are employed in the analysis because they require less computational effort compared to random field methods and are used to calculate the preliminary failure probability of a geotechnical system. The spatial variation of the geotechnical profile in tunnel stability analysis is incorporated utilizing the concepts of random field theories.

The limit analysis approach in the field of tunnel engineering has been broadly utilized to establish the limits of true collapse load of the system. This approach is mainly based on the lower and upper bound theorems of limit analysis (Chen and Liu 1990). The lower bound theorem states that if the equilibrium condition, stress boundary conditions, and yield criteria are satisfied, then the load determined from the stress distribution alone is less than the true collapse load. The upper bound theorem states that if the velocity boundary condition, strain and velocity compatibility are satisfied, then equating the external rate of work to the internal rate of dissipation in an assumed velocity field alone is not less than the true collapse load. The integration of limit analysis with random field concepts i.e., random finite element limit approach (RFELA) not only helps in determining the true collapse of the tunnel but also gives idea of statistical functions, namely, probability of failure, probability density function curves and cumulative distribution function curves (Ali et al. 2017; Cheng et al. 2019).

Although several probabilistic tunnel stability studies have been conducted to account for the inherent uncertainties associated with the geotechnical parameters, they do not consider the spatial variation of soil properties, e.g., Vargas et al. (2014). Few stability studies considering spatial variability are conducted considering the undrained behavior of soil (Ali et al. 2017), but tunnel stability studies in spatially variable cohesive frictional (c'-ϕ') soils are scarce.

In the current study, probabilistic stability analysis of tunnels in spatially variable cohesive frictional (c'-ϕ') lateritic soil is conducted, adopting the RFELA. In the study, effective cohesion (c'), effective friction angle (ϕ'), and unit weight of the soil (γ) are considered as random parameters. Firstly, a deterministic upper bound and lower bound tunnel collapse pressure are obtained. Random fields are generated using the KL expansion method. The output from the 1000 Monte Carlo simulations is then used to determine the probability density function (PDF) and the cumulative distribution function (CDF) of the collapse pressure of the tunnel. Parametric studies are conducted to study the effect of the coefficient of variation (COV) and correlation length (CL) on the failure probability (P_f). The RFELA results are then compared with those of Mondal and Tyagi's (2025a) random finite element analysis.

2 NUMERICAL MODEL

2.1 *Model Geometry and Material model*

A plane strain two-dimensional finite element model of a tunnel of diameter D, situated at cover depth C, is developed in Optum G2 (Figure 1). Left and right boundaries are fixed in the horizontal direction, and the bottom boundary is fixed in both vertical and horizontal directions. Model dimensions are kept as 11D in horizontal direction and 9D in vertical directions respectively. Model dimensions and mesh convergence studies are conducted so that any further change in the model dimensions and mesh size does not affect the results. The numerical model is discretized using 15-noded triangular elements. Model is discretized using with uniform mesh of 1m. The surrounding soil is modelled using the Mohr-Coulomb model. The finite element model shown in Figure 1 is used to perform both deterministic and random analyses.

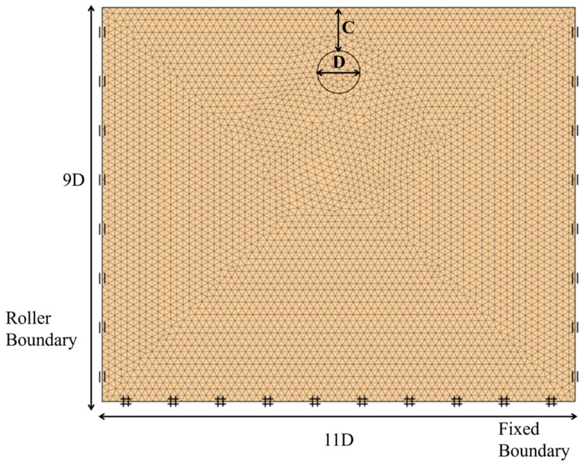

Figure 1. Plane strain finite element model with mesh and boundary conditions.

2.2 *Calculation of collapse pressure*

The tunnel construction is simulated by deactivating the soil cluster and uniform pressure of magnitude γ(C+D/2) inside the tunnel. Deterministic upper bound and lower bound tunnel collapse pressures (p) are determined by applying a multiplier load of unit magnitude.

2.3 *Generation of random fields*

Several methods are proposed in the literature for the generation of random fields, such as Covariance matrix decomposition method (Fenton and Griffiths 2008), Karhunen-Loeve expansion (KL) expansion method (Phoon et al. 2002), modified linear estimation method (Liu et al. 2014), etc. The choice of method depends on the computational efficiency available and the degree of accuracy required. The generation of random fields makes use of the mean (μ), the coefficient of variation, and the correlation length of the random parameters. CL tells about the distance at which the geotechnical parameters are correlated.

In this paper, the spatial variation of the geotechnical parameter is modelled using KL expansion method by generating the spatially correlated random fields of c', ϕ' and γ. The random parameters are assumed to be following the log normal distribution. Assumption of log normal distribution ensures non-negative values of the considered random parameter (Zhang et al. 2023). For a log normally distributed random parameter (say c'), if $\mu_{c'}$ represents its mean, $\sigma_{c'}$ represents its standard deviation and $COV_{c'}$ is its coefficient of variation, then the equivalent parameters of the normally distributed lnc' are $\mu_{lnc'}$ and $\sigma_{lnc'}$ (i.e., the mean and standard deviation of $ln_{c'}$) are:

$$COV_{c'} = \frac{\sigma_{c'}}{\mu_{c'}} \quad (1)$$

$$\sigma^2_{\ln c'} = \ln\left(1 + COV^2_{c'}\right) \quad (2)$$

$$\mu_{ln\, c'} = ln(\mu_{c'}) + \frac{1}{2}\sigma^2_{ln\, c'} \quad (3)$$

2.4 *Calculation of failure probability*

Several random simulations were performed using Monte Carlo in Optum G2. To determine the number of optimum Monte Carlo runs, a convergence study has been conducted using the cumulative mean and mean of p/c'. Figure 2 shows that 1000 Monte Carlo runs are sufficient to carry out further study, as convergence between the cumulative mean of normalized collapse pressure (p/c') and the mean of p/c' is achieved. Past studies have also shown that 1000 Monte Carlo simulations are sufficient to evaluate the P_f for tunnels in spatially variable media (Cheng et al. 2019; Zhang et al. 2022).

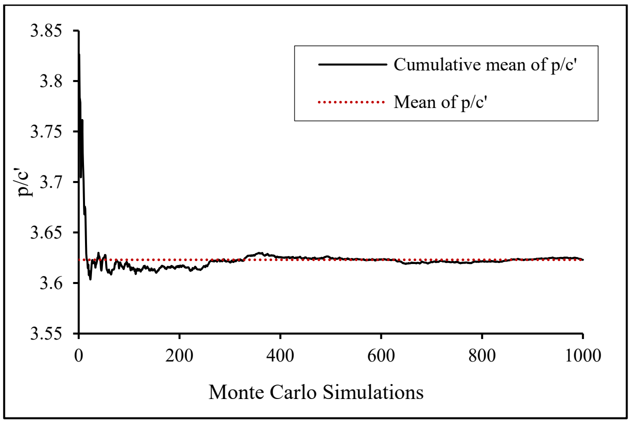

Figure 2. Plot of cumulative mean of p/c' Vs number of Monte Carlo runs.

Firstly, deterministic upper bound and lower bound tunnel collapse pressures are calculated for c' and ϕ' corresponding to 10 kPa and 22°, respectively. Thereafter, based on the normalised tunnel collapse pressure obtained from Monte Carlo simulations, P_f is calculated using the relation:

$$P_f = P\{(p/c')_{rand} \geq (p/c')_{det}\} \quad (4)$$

Here, $(p/c')_{det}$ and $(p/c')_{rand}$ are the deterministic normalized tunnel collapse pressure and the normalized tunnel collapse pressure obtained from a Monte Carlo simulation using random field theory.

Basically, P_f is calculated by dividing the number of tunnel collapse pressures obtained from a Monte Carlo simulation that are more than the deterministic tunnel collapse pressure by the total number of Monte Carlo runs (1000).

2.5 *Parametric studies*

Parametric studies are conducted to assess the effect of the statistical parameters, namely, COV, horizontal and vertical correlation length (CL_H and CL_V), on the P_f, PDFs and CDFs. The statistical and geotechnical parameters and their respective magnitudes considered in this study are listed in Table 1.

Out of the six cases mentioned in Table 2, the first 3 cases (1-3) correspond to a geotechnical profile having isotropic CL (CL_H = CL_V), and the next 3 cases (4-6) correspond to a geotechnical profile with anisotropic CL ($CL_H \neq CL_V$). Case 7 is considered for the comparison of the current study with the random finite element study of Mondal and Tyagi (2025a).

3 RESULTS AND DISCUSSION

Realization of random fields of c' corresponding to case 5 is shown in Figure 3. For the 20% $COV_{c'}$, the range of cohesion is from 5.99 kPa to 16.28 kPa. As CL_H is 20 times the CL_V, the uniformity of c' in horizontal direction is higher as compared to uniformity in vertical direction. Upper bound and lower bound P_f are calculated for 1000 Monte Carlo runs using Equation 4, and are reported in Table 3. Since the P_f for all cases is greater than 0.16, therefore safety level can be categorized as hazardous (USACE 1997).

Table 1. Statistical and geometrical parameters considered for the study.

Parameter	Magnitude	Reference
D (m)	6	-
C/D	1	-
$\mu_{c'}$ (kPa)	10	
$\mu_{\phi'}$ (°)	22	Chitra and Gupta (2016); Rahul and Tyagi (2025); Mondal and Tyagi (2025a)
μ_{γ} (kN/m³)	16	
$COV_{c'}$ (%)	10, 20, 40	
$COV_{\phi'}$ (%)	10	Phoon and Kulhawy (1999)
COV_{γ} (%)	10	
CL_V (m)	1,2	Viviescas et al. (2022)
CL_H/ CL_V	1, 20	

Table 2. Combination of statistical parameters for the study

Case No	$COV_{c'}$ (%)	$COV_{\phi'}$ (%)	COV_{γ} (%)	CL_V (m)	CL_H (m)
1	10	10	10	1	1
2	20	10	10	1	1
3	40	10	10	1	1
4	10	10	10	1	20
5	20	10	10	1	20
6	40	10	10	1	20
7	10	10	10	2	2

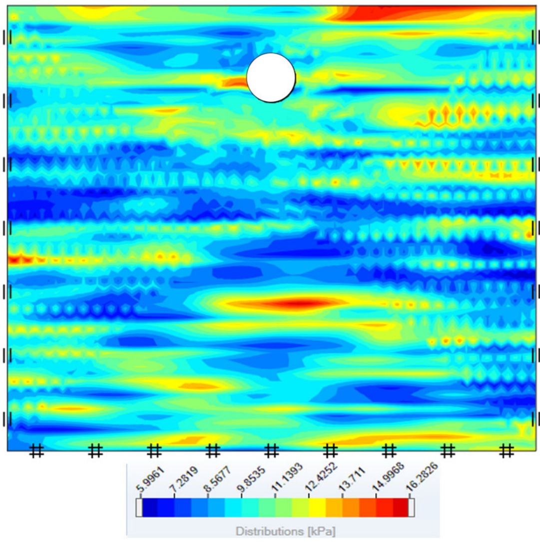

Figure 3. Realization of a random field of c' corresponding to case 5.

Table 3. Probability of failure for the cases 1 to 6.

Case No.	P_f (Lower bound)	P_f (Upper bound)
1	0.654	0.643
2	0.737	0.707
3	0.834	0.785
4	0.627	0.567
5	0.697	0.643
6	0.774	0.667

Figure 4 and Figure 5 show the PDFs and CDFs obtained for the normalized tunnel collapse pressure, respectively. The PDFs and CDFs will be helpful in accessing the probability density and P_f in the output p/c'.

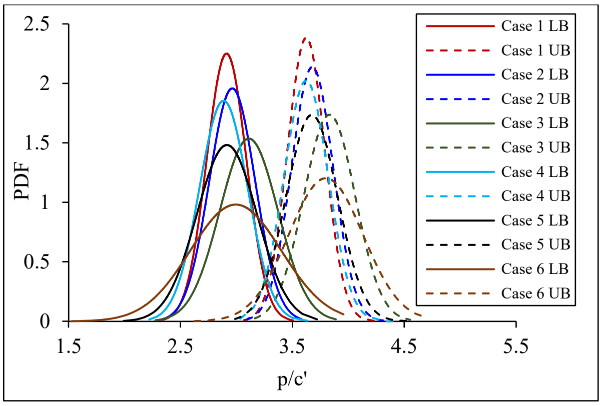

Figure 4. Upper bound (UB) and Lower Bound (LB) PDFs obtained from parametric studies.

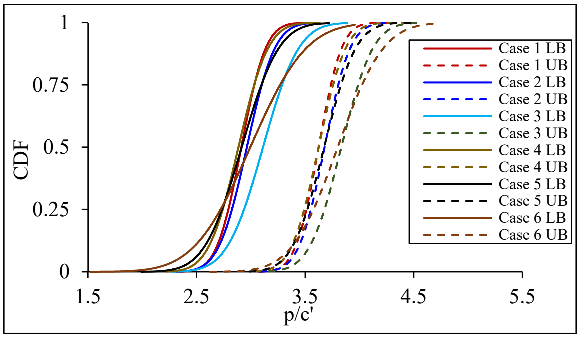

Figure 5. Upper bound (UB) and Lower Bound (LB) CDFs obtained from parametric studies.

3.1 *Effect of $COV_{c'}$*

It is inferred from Table 3, keeping the CL unchanged, with an increase in the $COV_{c'}$, an increase in the P_f is observed. If P_f for all three cases are compared, lower bound P_f for cases 1, 2 and 3 are 0.654, 0.737 and 0.834 respectively. A similar increase in P_f with $COV_{c'}$ is reported for the upper bound P_f. Similar observations are also reported for the cases of anisotropic CL. This is obvious as the tunnels in geotechnical profiles with high $COV_{c'}$ are more prone to failure than tunnels in geotechnical profiles with low $COV_{c'}$.

Comparison of PDFs of cases 1, 2, and 3 in Figure 4 shows that the peak for case 1 is highest, the lowest for case 3, and intermediate for case 2. On the one hand, the horizontal spread of PDF for case 1 is lowest, highest for case 3, and intermediate for case 2. PDFs are also seen to be shifting on the left-hand side, showing the increase in mean p/c' or decrease in stability of tunnels. Similar observations were also reported by Hamrouni et al. (2022). For cases 1, 2, and 3, the CDF of case 3 lies on the leftmost and case 1 lies on the rightmost. This indicates that the P_f of case 3 is higher than that of cases 1 and 2.

3.2 *Effect of horizontal and vertical CL*

Due to anisotropy and lower CL_V, the variability of c' is higher in the vertical direction as compared to the horizontal direction (Figure 3). As mentioned in Table 3, for the same $COV_{c'}$, P_f is found to be lower for cases of anisotropic CL as compared to cases of isotropic CL. As an illustration, the lower bound P_f for cases 1 and 4 are 0.654 and 0.627, respectively. This reduction can be attributed to an increase in the homogeneity of the geotechnical profile due to higher CL_H. The peaks of PDFs for cases of anisotropic CL are relatively lower as compared to cases of isotropic CL.

Table 4 shows the comparison between the current study and the RFEM-based study of Mondal and Tyagi (2025a). Both studies indicate that P_f is higher for isotropic CL as compared to anisotropic CL. The results of present RFELA study for $CL_H = CL_V = 2m$ are found to be approx. 15% lower than Mondal and Tyagi's (2025a) RFEM study. This may be attributed to the limitation of the RFELA study i.e. associated flow rule which is the underlying assumption of RFELA. The associated flow rule (dilation angle same as friction angle) leads to underestimation of critical tunnel support pressure (Mondal and Tyagi, 2025b). The second reason for the difference may be due to the method of obtaining the critical tunnel support pressure. Mondal and Tyagi (2025a) used the pressure-deformation approach for computing critical tunnel support pressure. Third reason may be the cross-correlation between the random parameters. However, the major advantage of using RFELA over RFEM is the less computational time and effort. RFEM study required approx. 5 hours for a single run, whereas in the present study, each run took only about 10 minutes, which is only approx. 3% compared to RFEM.

Table 4. Comparison of RFELA with those of RFEM.

Parameters	RFELA Current Study	RFEM Mondal and Tyagi (2025a)
CL_H=CL_V=2m	0.618 (LB), 0.611(UB)	0.725
CL_H=CL_V=1m	0.654 (LB), 0.643(UB)	-
CL_H=20m, CL_V=2m	-	0.567
CL_H=20m, CL_V=1m	0.627 (LB), 0.567(UB)	-

4 CONCLUSIONS

Based on the present study, following significant findings are obtained:

- For the given CL, P_f is found to increase with the increase in the $COV_{c'}$ due to an enhancement in the uncertainty associated with effective cohesion.
- P_f is observed to be higher for the cases of isotropic CL as compared to those of anisotropic CL.
- An increase in the $COV_{c'}$ of geotechnical parameters leads to a lower peak in the PDF and a wider horizontal spread, indicating greater variability in the output. The PDFs are found to be shifted to the right side with an increase in the COV of random parameters, indicating a reduction in tunnel stability with an increase in the COV of random parameters.
- The PDFs for the anisotropic CL are found to have a lower peak and wider horizontal spread compared to the cases of isotropic CL.
- The results of present RFELA study for $CL_H = CL_V = 2m$ are found to be approx. 15% lower than Mondal and Tyagi's (2025a) RFEM study. Despite the differences in the underlying assumptions and computation of critical tunnel support pressure in two methods, RFELA presents a fast and efficient way of finding the P_f of tunnel in spatially variable soils.

5 ACKNOWLEDGEMENT

The authors would like to acknowledge the financial support provided by Anusandhan National Research Foundation (ANRF), a statutory body of the Department of Science & Technology (DST), Government of India, under the Science & Engineering Research Board (SERB) competitive Core Research Grant Scheme, Grant Code No. SER-2040-CED (CRG/2022/003415) for conducting this study. The authors would like to thank the MHRD, Government of India, for providing scholarship to the first author for his doctoral program.

6 REFERENCES

Ali, A., Lyamin, A.V., Huang, J., Sloan, S.W., and Cassidy, M.J. 2017. Undrained stability of a single circular tunnel subjected to surcharge loading. *Computer and Geotechnics* 84, 16-27.

Campbell, J.B. 1979. Spatial variability of soils. Annals of the *Association of American Geographers* 69(4), 544-556.

Chen, W.H., and Liu, X.L. 1990. *Limit analysis in soil mechanics*. Developments in Geotechnical Engineering, New York USA Elsevier Science Publishers.

Cheng, H.Z., Chen, J., Chen, R.P., and Chen, G.L. 2019b. Reliability study on shield tunnel face using a random limit analysis method in multilayered soils. *Tunnelling and Underground Space Technology* 84, 353-363.

Chitra, R., and Gupta, M. 2016. Geotechnical investigations and slope stability analysis of a landslide. *International Journal of Engineering Research & Technology* 5(2), 120-127.

Curran, J.H. and Hammah, R. E. 2006. Keynote lecture: seven lessons of geomechanics software development. *Proc. 41st International Symposium on Rock Mechanics,* Colorado.

Fenton, G.A and Griffiths D.V. 2008. *Risk assessment in geotechnical engineering*. John Wiley & Sons, Inc. New Jersey.

Hamrouni A., Dias D., and Guo, X. 2022. Behavior of shallow circular tunnel -impact of soil spatial variability. *Geosciences* 12, 97.

Imteyaz, W., and Mishra, S. 2023. Failure of tunnels across the world: Case study. In: Expanding Underground - Knowledge and Passion to Make a Positive Impact on the World, Taylor and Francis

Liu, Y., Lee, F.H., Quek, S.T., and Beer, M. 2014. Modified linear estimation method for generating multi-dimensional multi-variate Gaussian field in modelling material properties. *Probabilistic Engineering Mechanics* 38, 42-53.

Low, B.K., and Einstein, H.H. 2013. Reliability analysis of roof wedges and rockbolt forces in tunnels. *Tunnelling and Underground Space Technology* 38, 1-10.

Mondal, S., and Tyagi, A. 2025a. Probabilistic analysis of tunnel stability in spatially variable cohesive-frictional soil. *Proc. 9th International Symposium for Geotechnical Safety and Risk,* Oslo, Norway.

Mondal, S., and Tyagi, A. 2025b. FEM-based pressure-deformation approach for determination of critical tunnel support pressure for tunnels in soils. In: Premalatha, K., Maji, V.B., Muttharam, M., Robinson, R.G (eds). *Women Indian Geotechnical Conference*. Chennai, March 8-9, 2024. Springer.

Phoon, K.K., and Kulhawy, F. H. 1999. Characterization of geotechnical variability. *Canadian Geotechnical Journal* 36, 612-624.

Phoon, K.K., Huang, S.P., and Quek, S.T. 2002. Simulation of second-order processes using Karhunen–Loeve expansion. *Computers and Structures* 80, 1049-1060.

Rahul, S., and Tyagi, A. 2025. Physics-based time-of-failure determination of rainfall-induced instability in lateritic soil slopes. *Engineering Geology* 344, 107834.

Sloan, S. W., and A. Assadi, A. 1993. Stability of shallow tunnel in soft ground. *Proc. Conference on Predictive Soil Mechanics* Thomas Telford, London 644-663.

USACE 1997. Risk-based analysis in geotechnical engineering for support of planning studies: Engineering and Design. US Army Corps of Engineers, Department of Army, Washington, DC, 20314-100.

Vargas, J.P., Koppe, J.C., and Perez S. 2014. Monte Carlo simulation as a tool for tunnel planning. *Tunnelling and Underground Space Technology* 40, 203-209.

Viviescas, J.C., Griffiths, D.V., and Osorio, J.P. 2022. Geological influence on the spatial variability of soils. *International Journal of Geotechnical Engineering.* 16(3), 382-390.

Zhang, J., Yang, J., Yang, F., Zhang, X., and Zheng, X. 2016. Upper-bound solution for stability number of elliptical tunnel in cohesionless soils. *International Journal of Geomechanics* 17(1), 06016011.

Zhang, Y., Liu, X., Yuan, S., Zhang, T., Song, J., and Chen W. 2022 Probabilistic stability analysis of qanat tunnels in c-ϕ soil considering soil spatial variability. *European Journal of Environmental and Civil Engineering* 27(12), 3763-3783.

Zhang, J., Xiao, T., Jian J., Peng, Z., and Cao, Z. 2023. Geotechnical Reliability analysis, Theories, methods and algorithms. *Springer*. Singapore